Prediction of *in Vivo* Tissue Distribution from *in Vitro* Data. 3. Correlation between *in Vitro* and *in Vivo* Tissue Distribution of a Homologous Series of Nine 5-n-Alkyl-5-Ethyl Barbituric Acids

Peter Ballard,[1,4] David E. Leahy,[2] and Malcolm Rowland[3]

Received February 13, 2003; accepted March 3, 2003

Purpose. To evaluate the ability to determine accurate *in vivo* tissue-to-unbound plasma distribution coefficients (Kpu_e) from *in vitro* data.

Methods. Fresh pieces of fifteen rat tissues/organs were incubated at 37°C with a homologous series of nine barbiturates covering a wide range of lipophilicity (Log P 0.02 to 4.13). Steady-state *in vivo* Kpu_e values were estimated from the tissue and plasma concentrations following simultaneous dosing by constant rate i.v. infusion of all nine barbiturates. Drug concentrations in the tissues and media were determined by HPLC with UV or mass spectrometric detection.

Results. The pharmacokinetics of the barbiturate series following constant rate i.v. infusion indicated a range of clearance (0.49 to 30 $ml.min^{-1}.kg^{-1}$) and volume of distribution at steady state (0.51 to 1.9 $l.kg^{-1}$) values. Good agreement was observed between the *in vitro* and *in vivo Kpu* values, although for the most lipophilic barbiturates the *in vitro* data underpredicted the *in vivo* tissue distribution for all tissues.

Conclusions. The *in vitro* system for predicting the extent of *in vivo* tissue distribution works well for compounds of widely differing lipophilicity, although for the most lipophilic drugs it may result in an underprediction of *in vivo* values.

KEY WORDS: *in vitro-in vivo* correlation; barbiturate; tissue distribution; pharmacokinetics.

INTRODUCTION

A partition coefficient is the ratio of the concentrations of a compound in two dissimilar media or phases at equilibrium. Tissue-to-plasma distribution coefficients (Kp) form an important component of many physiologically based mathematical models (1) that are used to both describe and predict the pharmacokinetics of compounds in animals and humans (2–4). *Kp* values have been estimated from *in vivo, in situ* and *in vitro* studies, although there are problems associated with each approach. *In vivo* studies are often conducted using i.v. bolus dosing (5,6) which, for compounds that are rapidly cleared from the body, can pose problems in the estimation of plasma and tissue AUCs and hence in *Kp* (7). A more appropriate *in vivo* technique is constant-rate i.v. infusion to steady state, where *Kp* is determined directly from the plateau tissue and plasma concentrations (3). *In situ* rat tissue preparations have also been utilized to investigate the uptake of drugs from perfusate (8–10). All these techniques generally require a substantial number of animals, skilled personnel and expensive equipment. Therefore, it would appear prudent to investigate the use of *in vitro* techniques as these are inexpensive to perform, require few animals and are less technically demanding.

The *in vitro* distribution or binding of drugs to tissues has been determined using homogenates (6,11), slices (12) and isolated tissue components (13). Of these preparations, tissue homogenates have been the most widely used but suffer from the inherent problem of disruption of cellular integrity. Consequently, for drugs exclusively or predominantly restricted to the extracellular space *in vivo*, the measured *in vitro Kp* will substantially overestimate the actual *in vivo* tissue distribution, because the total aqueous phase and intracellular binding sites are rendered accessible. *In vitro* drug distribution studies have been conducted using tissue slices or pieces to maintain a greater degree of tissue integrity than seen with homogenates (12,14–16). In previous reports (17,18) we critically examined an *in vitro* model of tissue distribution that involves the use of tissue pieces, using marker compounds for extracellular and total tissue water spaces.

The aims of this study were to apply this *in vitro* model of tissue distribution to a homologous series of nine 5-n-alkyl-5-ethyl barbituric acids and to compare *Kpu* values with those obtained *in vivo* following constant-rate i.v. infusion. A secondary objective was to compare the constant-rate findings with those obtained previously following an i.v. bolus dose of these barbiturates in the rat (7). This homologous series spans a range of lipophilicity typical for drug molecules (Table I) and, with all homologues having a pKa of approximately 7.8 (19), they are essentially unionized at physiologic plasma pH.

MATERIALS AND METHODS

Reagents

All chemicals were of analytical reagent grade unless otherwise stated. Hanks' Balanced Salt Solution (containing D-glucose, HBSS) was supplied by Life Technologies Limited, Paisley, UK. Amylobarbital, phenobarbital, thiopental, 5,5-diethyl, and 5-n-butyl-5-ethyl barbituric acids were obtained from Sigma Chemical Company Ltd., Poole, Dorset, UK, 5-n-pentyl-5-ethyl barbituric acid was a gift from Zambon Group spa, Bresso, Milan, Italy, with the remaining 5-alkyl-5-ethyl barbituric acids (methyl, n-propyl, n-hexyl, n-heptyl, n-octyl, and n-nonyl) synthesized in the School of Pharmacy and Pharmaceutical Sciences, University of Manchester, Manchester, UK and purified to greater than 95% as estimated by micro-analysis (19). The n-nonyl derivative was prepared as the sodium salt. Hydroxypropyl β-cyclodextrin (average molecular weight 1380) and 4-(2-hydroxyethyl)-1-piperazineethanesulphonic acid, sodium salt (HEPES) were supplied by Aldrich Chemical Company, Gillingham, Dorset, UK. Acetonitrile (far UV grade), methyl tertiary-butyl ether (MTBE), potassium dihydrogen orthophosphate, and disodium hydrogen orthophosphate (anhydrous)

[1] Discovery-DMPK, Mereside, AstraZeneca, Alderley Park, Cheshire, SK10 4TG, United Kingdom
[2] Cyprotex, 15 Beech Lane, Macclesfield, Cheshire, SK10 2DR, United Kingdom
[3] School of Pharmacy and Pharmaceutical Sciences, University of Manchester, Manchester, M13 9PL, United Kingdom.
[4] To whom correspondence should be addressed. (e-mail peter.ballard@astrazeneca.com)

0724-8741/03/0600-0864/0 © 2003 Plenum Publishing Corporation

Table I. Molecular Weight, Dissociation Constant (pKa), Lipophilicity ($LogP_{octanol/water}$), Fraction Unbound in Rat Plasma (fu) and Whole Blood-to-Plasma Concentration Ratio (R) of the 5-n-Alkyl-5-Ethyl Barbituric Acids

Barbituric acid homologue	Molecular weight	pKa[a]	LogP[b]	fu[a]	R[a]
methyl	170.2	8.11	0.02[a]	1	0.93
ethyl	184.2	7.75	0.68[c]	0.95	0.97
n-propyl	198.2	7.77	0.87	0.88	0.97
n-butyl	212.2	7.81	1.70	0.61	1.42
n-pentyl	226.2	8.00	2.20	0.51[d]	
n-hexyl	240.2	7.74	3.08	0.19	1.00
n-heptyl	254.2	7.78	3.64	0.061	0.98
n-octyl	268.2	7.78	3.85	0.026	1.08
n-nonyl	282.2	7.82	4.13	0.0093	1.05

[a] (19).
[b] (30).
[c] (31).
[d] Estimated from the percentage bound versus LogP relationship for the barbiturates (19).

were supplied by Fisons Scientific Equipment Loughborough, Leicestershire, UK. Hanks/HEPES buffer was prepared by adding HEPES to HBSS at 10 mM. Hydroxypropyl β-cyclodextrin was prepared as a 15% aqueous solution (w/v).

Dose Solutions for the Constant-Rate I.V. Infusion Study

Two dose solutions (15% aqueous hydroxypropyl β-cyclodextrin) were required for the study containing a mixture of barbituric acids at concentrations detailed in Table II: 1; methyl to n-pentyl analogues for the bolus dose and 2; methyl to n-nonyl analogues for the constant-rate infusion dose. Both solutions were filtered through a 0.45 μm filter prior to dosing.

Surgery

Fifteen male Wistar derived rats (approximately 250 g) were each fitted with an indwelling cannula into the vena cava by way of the femoral vein under halothane anesthesia 7 to 9 days prior to dosing. The cannula were exteriorized by way of the tail cuff and swivel mechanisms to allow the animals total movement around the cage. All animals received a constant-rate i.v. infusion of physiologic saline (using a Secura FT perfusor manufactured by B. Braun, Germany) by way of the cannula at approximately 5 $ml.h^{-1}.kg^{-1}$ from surgery until dosing.

Live Phase

The rats were administered with an i.v. bolus dose (2 $ml.kg^{-1}$) followed immediately by a constant-rate i.v. infusion (5 $ml.h^{-1}.kg^{-1}$) of barbituric acid solutions. Blood samples (0.5 ml) were taken from a tail vein at various times up to sacrifice aimed at rapidly achieving a steady state in plasma and tissues. Rats were sacrificed by cervical dislocation after 3, 6, or 9 h (n = 4 at each time point). The designated tissues, see Table III were removed immediately after sacrifice and stored at –20°C until analyzed. The stomach and intestine samples were washed with physiologic saline and blot dried prior to storage. All samples were analyzed by HPLC-MS-MS.

In Vitro Tissue Distribution

The *in vitro* tissue distribution study was conducted with fresh rat tissue pieces (Table IV) cut freehand with scissors (approximately 50 mg), accurately weighed and incubated with Hanks/HEPES buffer (2 ml, containing methyl to n-nonyl barbituric acids each at 50 $nmol.ml^{-1}$) in a shaking waterbath at 37°C. At times up to 6 h, tissue samples were removed, blot dried and reweighed. Tissue and medium samples were analyzed by HPLC-UV.

Sample Extraction

Rat tissues samples (40–100 mg) were homogenized with phosphate buffer (3 ml, 0.07 M, pH5.4) and the barbiturates extracted into MTBE (5 ml). After evaporation, the MTBE residues were redissolved in methanol:water (0.2 ml, 1:1 v/v) or acetonitrile:water (0.2 ml, 1:1 v/v) for analysis by HPLC-UV (*in vitro* study) or HPLC-MS-MS (*in vivo* study), respectively.

Table II. Bolus and Infusion Dose Solution Concentrations for the Current Study and Pharmacokinetic Parameters for the 5-n-Alkyl-5-Ethyl Barbituric Acid Derivatives Estimated following Constant-Rate Infusion and a Previous i.v. Bolus (19) Studies

Barbituric acid homologue	Concentration of dosing solutions ($\mu mol.ml^{-1}$)		C_{9h} (±SE) ($nmol.ml^{-1}$)	CL (infusion) ($ml.min^{-1}.kg^{-1}$)	CL (bolus) ($ml.min^{-1}.kg^{-1}$)	V_{ss} (infusion) ($l.kg^{-1}$)	V_{ss} (bolus) ($l.kg^{-1}$)
	Bolus	Infusion					
methyl	4.26	0.115	8.3 (±0.62)	1.2	1.46	0.57	1.82
ethyl	3.80	0.051	8.6 (±0.54)	0.49	0.85	0.51	1.00
n-propyl	4.88	0.063	8.9 (±0.42)	0.58	0.97	0.56	1.34
n-butyl	2.21	0.043	1.6 (±0.071)	2.3	3.7	0.68	1.21
n-pentyl	4.47	0.796	7.7 (±0.31)	8.7	8.4[a]	0.74	1.64[b]
n-hexyl	0[a]	1.47	6.4 (±0.73)	19	24.4	0.94	0.88
n-heptyl	0[a]	1.62	4.2 (±0.74)	33	25.8	1.1	0.78
n-octyl	0[a]	1.94	3.9 (±0.85)	42	35.1	1.4	0.88
n-nonyl	0[a]	2.01	5.7 (±0.92)	30	32.3	1.9	1.23

[a] No bolus loading dose given.
[b] iso-Pentyl rather than n-pentyl barbituric acid was studied in the i.v. bolus study (19).
C_{9h} = Plasma concentration after 9 h infusion.
V_{ss} was estimated from Eq. 3.

Table III. Mean Tissue-to-Unbound Plasma Distribution Coefficients (Kpu_e) for 5-n-Alkyl-5-Ethyl Barbituric Acid Homologues in Rat Tissues Determined after 9 h Constant-Rate i.v. Infusion

Tissue	methyl	ethyl	n-propyl	n-butyl	n-pentyl	n-hexyl	n-heptyl	n-octyl	n-nonyl
Adipose, abdom	0.15	0.21	0.49	1.6	3.3	17	60	225	737
Adipose, brown[a]	0.64	0.62	0.81	1.5	2.1	8.0	26	100	265
Adipose, subcut	0.24	0.29	0.54	1.5	3.0	16	56	214	774
Brain	0.67	0.67	0.78	1.5	1.8	6.3	21	79	272
Heart	0.83	0.82	1.1	1.8	1.8	5.6	18	52	122
Intestine	0.54	0.52	0.78	1.2	1.4	4.4	14	47	202
Kidney	1.3	1.7	2.3	3.9	4.5	13	33	98	210
Liver	0.80	0.77	1.1	2.4	3.4	21	58	290	723
Lungs	0.87	0.75	0.94	1.2	1.3	5.0	18	116	355
Muscle, abdom	0.58	0.54	0.62	0.94	1.1	3.2	9.0	30	84
Muscle, back	0.64	0.57	0.66	1.1	1.3	4.0	10	32	78
Muscle, thigh	1.1	0.90	0.98	1.5	1.7	5.7	16	51	124
Pancreas	0.67	0.63	0.91	1.8	2.2	8.4	26	88	283
Skin	0.53	0.51	0.70	1.4	2.2	9.2	32	117	390
Spleen	0.70	0.55	0.61	0.59	0.66	4.4	19	72	332
Stomach	0.58	0.54	0.74	1.3	1.7	6.2	21	68	263
Testes	0.64	0.58	0.73	1.2	1.2	3.9	13	43	130
Thymus[a]	0.75	0.74	0.90	1.3	1.1	2.6	8.1	34	93

[a] Values uncorrected for amount of barbiturate in tissue vasculature. abdom = abdominal, subcut = subcutaneous.

HPLC-UV Conditions

All barbiturates and the internal standard (amylobarbital) were simultaneously analyzed using a Hypersil ODS 5 μm (250 × 4.6 mm I.D.) column with a linear gradient operating from 15:85 to 90:10 acetonitrile:water (containing 0.1% trifluroacetic acid) at 1.0 $ml.min^{-1}$ and the eluent monitored at 214 nm. The assay limit of detection was 5 $nmol.g^{-1}$ of tissue, and the imprecision was typically less than a coefficient of variation of 10% for all barbiturates.

HPLC-MS-MS Conditions

All barbiturates (including phenobarbital as the internal standard) were simultaneously analyzed using a Hypersil C18BDS 3 μm (150 × 0.3 mm I.D.) column at 35°C, an acetonitrile:deionized water (75:25 v/v) mobile phase operated at a flow rate of 150 $\mu l.min^{-1}$ and split to allow 4.5 $\mu l.min^{-1}$ to flow to the detector. The mass spectrometer conditions used were negative electrospray ionization with the $(M\text{-}H)^-$ to m/z 42 $(CNO)^-$ ions monitored for all barbituric acids, 43 eV collision energy and 25 V cone voltage. All 11 channels were measured consecutively, with a 0.2 s dwell time and 0.02 s interchannel delay. The limit of detection was approximately 0.5 $nmol.g^{-1}$ of tissue and the imprecision was typically less than a coefficient of variation of 15%.

Calculations

In Vivo

The pharmacokinetic parameters have been calculated using standard methods.

Table IV. Mean Tissue-to-Unbound Plasma Distribution Coefficients (Kpu_e, Corrected for Swelling and Barbiturate in the Vasculature) for 5-n-Alkyl-5-Ethyl Barbituric Acid Homologue in Rat Tissues Determined After 5 h *in Vitro* Incubation

Tissue	Swelling (%)	methyl	ethyl	n-propyl	n-butyl	n-pentyl	n-hexyl	n-heptyl	n-octyl	n-nonyl
Adipose	39.5	0.25	0.44	0.75	1.8	4.9	15	33	57	55
Brain	34.5	0.87	1.03	1.1	1.6	3.0	7.0	14	23	28
Heart	8.8	0.65	0.80	1.2	1.8	3.7	9.2	20	33	48
Intestine	–0.9	0.79	0.86	1.0	1.4	2.3	6.0	12	16	14
Kidney	33.8	0.72	0.89	1.2	1.8	3.3	8.0	17	26	34
Liver	20.8	0.95	1.0	1.3	2.0	4.2	10	22	35	44
Lungs	56.8	0.65	0.71	0.92	1.5	3.2	8.3	19	34	53
Muscle	48.1	0.58	0.70	1.0	1.3	2.3	5.4	12	21	31
Pancreas	22.6	0.17	0.35	0.7	2.0	6.3	20	49	94	108
Skin	31.7	0.53	0.72	0.94	1.4	2.8	6.6	13	19	22
Spleen	8.7	0.54	0.66	0.89	1.5	2.9	7.1	16	27	42
Stomach	6.1	0.69	0.80	1.0	1.5	2.7	6.0	12	15	13
Testes[a]	–12.5	0.81	0.91	1.0	1.3	2.0	4.1	9.0	14	15
Thymus	5.2	0.64	0.74	0.90	1.3	2.6	6.5	15	24	29

[a] Due to some loss of tissue during the incubation, the testes Kpu_e values were calculated using the swollen tissue weight and could not be corrected for swelling.

The tissue-to-unbound plasma distribution coefficients (Kpu_e) of the barbituric acids were calculated by correcting for the amount of blood in the tissue (Eq. 1); i.e., tissue is defined as not including blood.

$$Kpu_e = \frac{Kp_e}{fu} = \frac{(A_T - A_{T,vas}) \,/\, W \cdot (1 - f_{vas})}{C \cdot (1 - E_i)} \quad (1)$$

where A_T and $A_{T,vas}$ are the total and vascular amounts of barbituric acids in tissue samples respectively, W is the tissue weight, f_{vas} is the vascular fraction of the tissue (3), fu is the fraction unbound in plasma (Table I) and E_i is the organ extraction ratio. The amounts of barbiturate in thymus and brown adipose tissue were not determined as reliable estimates of their vascular fraction could not be found.

The amount of barbiturate in the vascular compartment was estimated from Equation 2, by assuming that for eliminating tissues the amount was derived from the mean concentration entering and leaving the tissue.

$$A_{T,vas} = C\left(1 - \frac{E_i}{2}\right) \cdot R_b \cdot W \cdot f_{vas} \quad (2)$$

where R_b is the blood-to-plasma concentration ratio.

The volume of distribution at steady state (V_{ss}) was estimated from the tissue distribution coefficient data as described in Eq. 3, where V_b and $V_{T,i}$ are the total blood volume and the anatomic volume of the i^{th} tissue (3) respectively.

$$V_{ss} = V_b + \sum V_{T,i} \times Kp_{e,i}\,(1 - E_i) \quad (3)$$

The tissue distribution half life ($t_{1/2T}$) was estimated from Eq. 4, where Q_T is the blood flow to the tissue.

$$t_{1/2T} = \frac{0.693 \cdot Kp_e}{Q_T \,/\, V_T} \quad (4)$$

In Vitro

The tissue-to-medium distribution coefficient (Kpu) following an *in vitro* incubation was calculated directly from the barbituric acid concentration in tissue (C_T) and in the medium (C_M) at the end of the incubation, Eq. 5.

$$Kpu = \frac{C_T}{C_M} \quad (5)$$

Since tissue slices swell during an *in vitro* incubation (18), the Kpu has to be corrected for the barbiturate imbibed in buffer and in the vascular space, Kpu_e:

$$Kpu_e = \frac{(A_T - A_{T,imb} - A_{T,vas})}{C_M \cdot W \cdot (1 - f_{vas})} \quad (6)$$

where $A_{T,imb}$ is the additional amount of barbiturate in the tissue at the end of the incubation resulting from imbibed medium, calculated by assuming that the barbiturate concentration in imbibed medium was equal to that in the bulk medium at the end of the incubation. Due to disintegration of testes tissue during the incubation, Kpu_e was calculated using the swollen tissue weight (18).

For simplicity, the terms $Kp_e(t)$ and $Kpu_e(t)$ are used to designate the tissue-to-plasma or unbound plasma distribution coefficients measured at times up to equilibrium.

The *in vitro* distribution of compounds can also be affected by the loss of albumin from tissue pieces into the incubation medium (17). This has been assessed for the barbiturate series using the following equation, utilizing experimentally determined or readily available parameters (17,19):

$$Kpu = Kpu_{app}\left[1 + \theta_E\left(\frac{V_T}{V_M}\right) \cdot \left(\frac{1 - fu}{fu}\right) f_p\,(1 - f_R)\right] + \frac{\theta_E(1 - f_R)\left(\frac{1 - fu}{fu}\right) f_P}{Kpu_{app}} \quad (7)$$

where Kpu_{app} is the measured *in vitro* tissue-to-unbound plasma partition coefficient, $\theta_E = V_E/V_T$ (V_E and V_T are the extracellular and total tissue volumes respectively); V_M, the volume of incubation medium; f_R, fraction of extracellular binding protein remaining in tissue at the end of the incubation, f_P, the ratio of the total binding protein concentrations originally in extracellular space to that in plasma.

Statistics

The *in vitro* and *in vivo* Kpu_e values were compared using a two-sample student's group t test, assuming that the means of both data sets are equal with a 95% confidence level. Statistical significance was assumed for a probability (p) of <0.05.

RESULTS

Constant-Rate I.V. Infusion

At the end of the infusion (9 h) the barbituric acids plasma concentrations ranged from 1.6 to 8.9 nmol.ml^{-1}, Table II. The estimated plasma clearances (CL) ranged from 0.49–42 ml.min.$^{-1}$kg^{-1} and the volume of distribution at steady state (V_{ss}) from 0.51–1.9 l.kg^{-1} (Table II). The plasma and tissue concentrations (Fig. 1) indicated that steady state had been achieved within 9 h infusion.

The Kpu_e values ranged from 0.15 to 774 for methyl to n-nonyl barbituric acids in adipose tissue, the most sensitive tissue to increasing barbiturate lipophilicity, and from 0.54 to 124 in muscle, the least sensitive tissue (Table III). The mean Kpu_e coefficient of variation (CV) in all tissues varied from 21% (range 1–71%) for methyl barbituric acid to 44% (14-75%) for the n-octyl homologue.

The individual barbituric acid Kpu_e values are generally not dependent on the site from which a tissue was sampled. Hence, for the barbiturates a significant difference between Kpu_e in abdominal and subcutaneous adipose tissues was only observed for the ethyl and n-propyl homologues ($p = 0.016$ and 0.037, respectively). There was no significant difference between Kpu_e values for any barbiturate when using samples of abdominal, back, or thigh muscle.

In Vitro Tissue Distribution

The *in vitro* barbituric acid Kpu_e values at incubation times up to 6 h are illustrated for adipose tissue and muscle in Fig. 2. In both tissues, there was an initial rapid increase in measured Kpu_e over the first 15 min, followed by a slower phase reaching equilibrium after approximately 3 h. The barbiturate Kpu_e values measured in rat tissues ranged from 0.17–0.95 for the methyl homologue and 13–108 for the n-nonyl derivative, with CVs typically less than 30%. In addi-

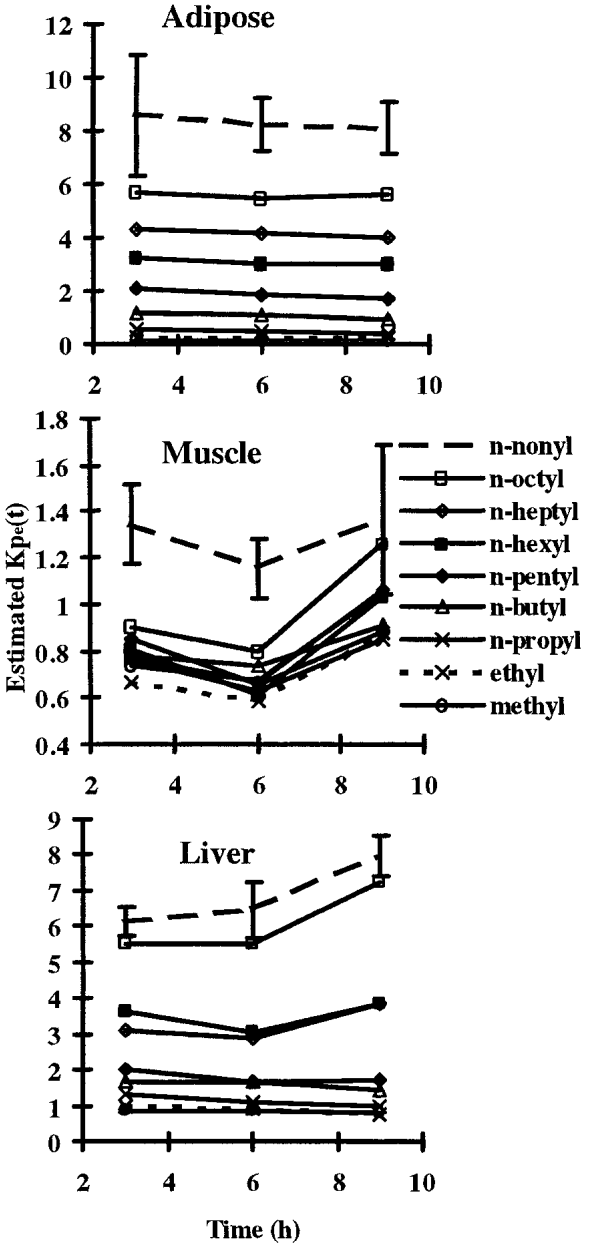

Fig. 1. Mean (n = 4) estimated barbituric acid $Kp_e(t)$ values in abdominal adipose tissue, thigh muscle, and liver after 3, 6, and 9 h constant-rate i.v. infusion. The mean $Kp_e(t)$ values are indicated as data points and the lines simply connect these values. Standard error bars are included for the n-nonyl homologue to indicate the general degree of variability in estimating $Kp_e(t)$ values.

tion, barbiturate Kpu_e values generally increased with increasing compound lipophilicity.

The effect of albumin diffusion from tissue pieces into the incubation media on barbiturate *Kpu* was assessed using Eq. 7 and compared to alternate methods for muscle in Fig. 3. For the barbiturate series, the diffusion of albumin from the tissue pieces to media had a maximum effect of 20% on the estimated *Kpu* value, as observed for the n-nonyl homologue. A larger effect was observed by correcting for the excess amount of barbiturate in the tissue caused by swelling and the amount present in the vasculature.

There was a reasonable correlation (r^2 = 0.80) between

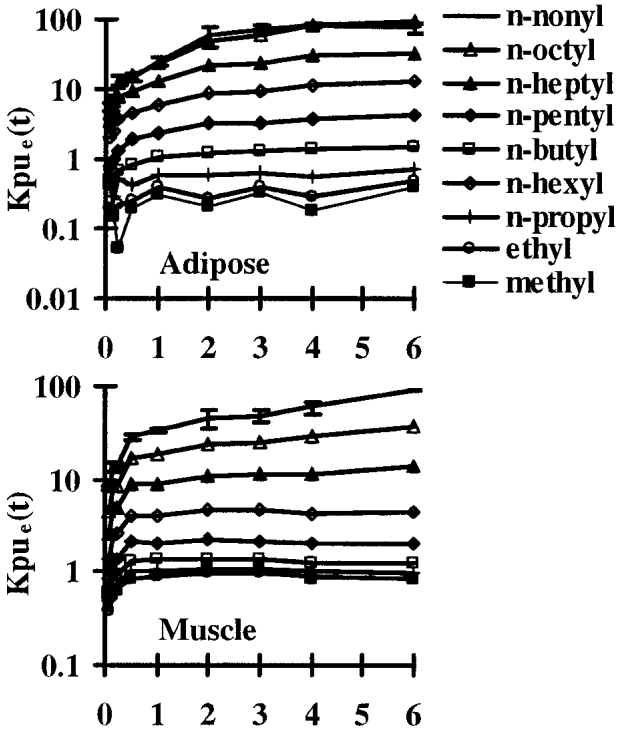

Fig. 2. Semilogarithmic plot of mean (n = 3) methyl to n-nonyl barbituric acid $Kpu_e(t)$ values in adipose tissue and muscle pieces during an *in vitro* incubation using tissue pieces (50 mg) and Hanks/HEPES buffer (2 ml) containing all the barbiturate series at 50 $nmol.ml^{-1}$. The lines comprise linear connections between consecutive data points for each of the barbiturates.

the Kpu_e estimated *in vitro* and *in vivo* by constant-rate i.v. infusion for the barbituric acid series (Fig. 4). In general the data lie close to the line of unity although clearly the n-octyl and n-nonyl homologues *in vitro* Kpu_e values underestimated those following i.v. infusion.

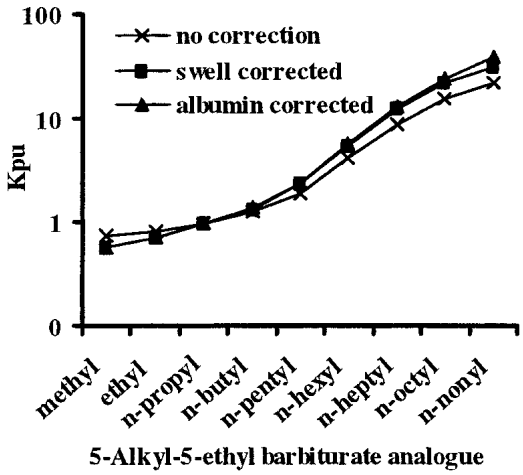

Fig. 3. Barbiturate *Kpu* values in muscle tissue using 3 estimation methods: 1. Without correcting for the increase in barbiturate tissue concentration caused by imbibed media during the incubation; 2. By correcting for barbiturate from imbibed media and in vascular space (Kpu_e); 3. By correcting for barbiturate bound to albumin diffusing from the tissue to the incubation media. The lines comprise linear connections between consecutive data points for each of the barbiturates.

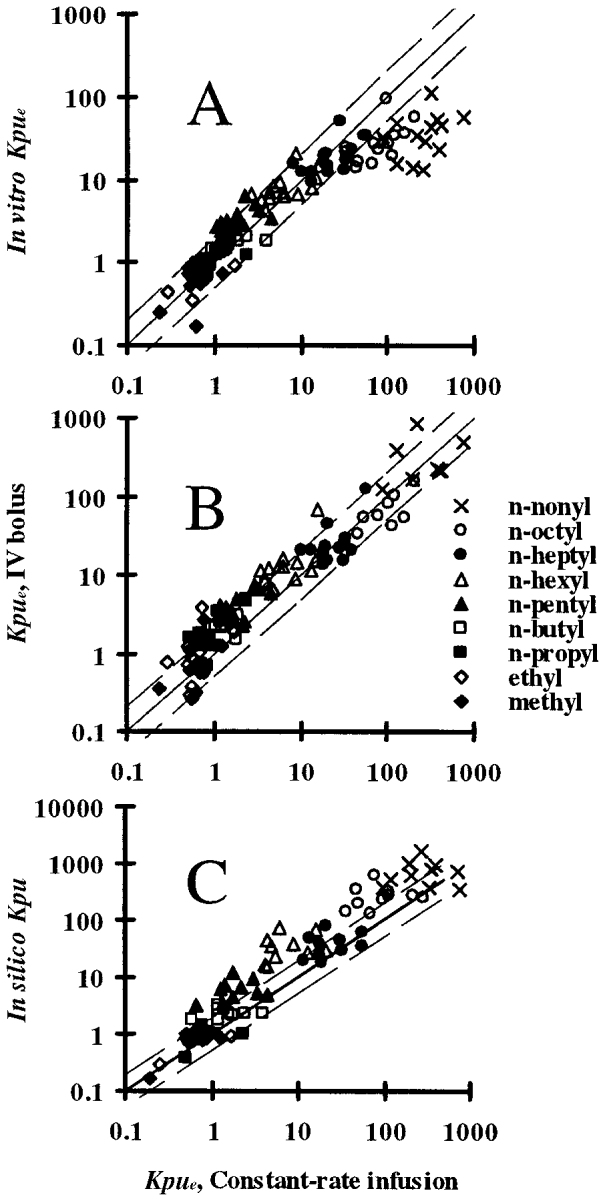

Fig. 4. Correlation between barbituric acid Kpu_e values determined from constant-rate i.v. infusion studies and: A. Estimated from *in vitro* incubations (5 h incubation and corrected for swelling and barbiturate in the vasculature); B. Estimated by i.v. bolus (7); and C. *In silico* prediction using LogP, pKa, and fraction unbound in plasma, by the method described by Poulin and Theil (27). Data are shown as points for individual barbituric acid homologues, the solid line shown is the line of unity and the dashed lines represent factors two above and two below the line of unity in all panels.

DISCUSSION

Experimental Design

The dosage schedules for the barbituric acids for the i.v. infusion study were based on a combination of the results from a pilot infusion study and simulations using previous i.v. bolus data (19,20). The aim was to achieve a steady state in plasma well within the 9 h study period, so as to maximize the chance of obtaining a true estimate of *Kpu*. When infused only the time to achieve steady state is primarily determined by the elimination half-life. The plasma half-lives of the n-hexyl to n-nonyl homologues are sufficiently short, 0.42–0.62 h (19), that steady state in plasma was predicted to be reached within 3 h of infusion. However, for the methyl to n-pentyl homologues, an i.v. bolus loading dose was required because the terminal half lives of these compounds are moderately long (2.4–17 h) compared to the time scale of the infusion.

To minimize the number of animals studied, all nine barbiturates were dosed simultaneously as a cocktail. The study was designed to achieve steady-state barbituric acid plasma concentrations of only 5 $nmol.ml^{-1}$, each after 9 h of infusion, to minimize any potential pharmacokinetic problems. The final plasma concentrations achieved (from 1.6–8.9 $nmol.ml^{-1}$) were generally within a factor of 2 of the predicted values.

Steady-State Considerations

The tissue distribution half life ($t_{1/2T}$, Eq. 4) provides a guide as to how quickly individual tissues would reach steady state, given a constant arterial concentration. Clearly this parameter depends on a good estimate of Kp_e, which by definition is a steady-state parameter. Its estimate also assumes that tissue distribution is perfusion rate limited, which appears the case for essentially all barbiturates and tissues (7). For the barbituric acid series the calculated values of $t_{1/2T}$ were all <1 h, except for the n-heptyl to n-nonyl homologues in adipose tissue (1.1–2.4 h). Therefore, the $t_{1/2T}$ values suggest that the barbituric acids should be close to, or at, equilibrium in the tissues well within the 9 h infusion period.

Pharmacokinetic Parameters

We do not believe that hydroxypropyl β-cyclodextrin, used to help solubilize the barbiturates in the infusion solution, materially affected the pharmacokinetics of the compounds. Certainly, the clearance estimates for all the barbituric acids agreed well (ranging from –42–+26%) with previous values after i.v. bolus dosing (19), supporting the view that these barbiturates were close to steady state in plasma after 9 h constant-rate infusion (Table II). There was a gradual trend in this study for volume of distribution at steady state (V_{ss}) to increase with increasing barbiturate lipophilicity that was not observed following i.v. bolus dosing (Table II). It is difficult to rationalize whether there is a true difference in V_{ss} between the studies or if this is purely down to the calculation method. For the more hydrophilic barbiturates, V_{ss} estimates were close to total body water, whereas preferential distribution into tissue components over plasma was apparent for the more lipophilic homologues (V_{ss} >1 $l.kg^{-1}$).

In Vivo Kpu_e Values

The correction of Kpu_e values to account for residual compound in blood within the tissue vasculature has a minimal effect for the barbiturates in most tissues. However, in highly vascularized tissues (e.g., lung and spleen) the correction often resulted in a 5–10% decrease in Kpu_e for the hydrophilic barbituric acids and a 10–20% increase for the most lipophilic homologues.

The Kpu_e results for methyl to n-pentyl barbituric acids in kidney were consistently greater than those in other tissues. This probably results from an overestimate of the barbiturate tissue concentrations due to the presence of these compounds

in the kidney tubule. Kpu_e values for adipose tissue and muscle were independent of the tissue sampling site, which is consistent with literature values for 5-ethyl-5-n-nonyl barbituric acid (21).

The Kpu_e values of this barbituric acids series generally agreed within a factor of two to three with those from an i.v. bolus dose (7), Fig. 4. However, the methyl to n-hexyl homologue Kpu_e values were generally overestimated by the i.v. bolus data and there were substantial discrepancies between some individual results. This may be a result of poor estimates of plasma and tissue AUC following i.v. bolus dosing due to the rapid elimination of the n-nonyl and n-octyl barbituric acid homologues. In contrast, *Kpu* can be readily determined from a single tissue and plasma sample when at steady state with a constant rate i.v. infusion study. Also, this latter approach is more analogous to the *in vitro* methodology.

In Vitro Kpu Values

The use of an optimum medium-to-tissue volume ratio is essential to obtaining Kpu_e values within a reasonable timescale. Consequently, preliminary experiments varying the mass of tissue pieces, the incubation time and the buffer were conducted. The final conditions used, 50 mg of tissue and 2 ml of buffer, were settled on because they were simple, ensured equilibrium was achieved within a reasonable timescale (4–5 h, Fig. 2) and the tissue pieces were sufficiently thin to allow oxygenation to help maintain cellular viability (14). With larger tissue pieces, it is likely that the center of the tissue will not be oxygenated sufficiently. Smaller pieces may result in analytical sensitivity issues and also a higher proportion of disrupted cells, both of which will affect the accuracy of the *Kpu* estimate.

There are two problems endemic to the *in vitro* incubation methodology used here: tissues swell with imbibed media (18) and albumin diffuses from the tissue to the media (17). For compounds that are not restricted to extracellular space (e.g. barbiturates) a simple correction can be made to the calculation of Kpu_e to account for the amount of compound associated with the imbibed media (Eq. 7). This correction can significantly affect the Kpu_e estimate, although the direction of the effect depends on the extent of tissue partitioning (Fig. 3). For example, by not accounting for barbiturate in imbibed media the Kpu_e in muscle tissue would be overestimated by approximately 25% for the n-methyl homologue but slightly underestimated (around 0.5%) for the n-nonyl homologue.

The diffusion of albumin from tissue pieces into incubation media can result in a large error in the *Kpu* estimation for drugs that are restricted to extracellular space and are highly bound to this plasma protein (17). This is because the drug concentrations in the media are now total rather than unbound values. This only results, however, in a minor increase in the *Kpu* value for the current barbiturate series, as illustrated for muscle tissue in Fig. 3.

In practice, both swelling and albumin diffusion occur simultaneously. Although this condition represents a complex picture that we have not combined within a model, it is clear that the *Kpu* values of hydrophilic molecules are overestimated if swelling is not accounted whereas the *Kpu* values of lipophilic, highly protein bound molecules are underestimated by albumin diffusion. For the current barbiturate series, tissue swelling had a more profound effect on *Kpu* values than albumin diffusion.

In Vitro to *in Vivo* Correlation

In vitro Kp values have been used in PBPK models (22,23) although there is only sparse information to indicate whether they are a good predictor of the corresponding *in vivo* values. Good *in vitro* to *in vivo* correlations have been observed for ethoxybenzamide, a neutral compound, in many tissues and for some anionic drugs in muscle, liver, lungs, and kidney, although there were marked differences for the lipophilic cations imipramine, propranolol, and quinidine (24–26).

The homologous set of barbiturates used in the current study represents a systematic approach to investigate *in vitro* tissue distribution by restricting changes in physicochemical properties to essentially lipophilicity alone. The correlation between the barbiturate *in vitro* and *in vivo* Kpu_e values indicates that it is possible to predict *in vivo* tissue distribution from the *in vitro* experiments for compounds having quite a wide range of lipophilicity (Fig. 4). It is unclear, however, why there would be such a divergence between *in vitro* and *in vivo* Kpu_e values for the most lipophilic barbiturates (twenty four out of twenty eight *in vitro Kpu* values were less than half the *in vivo* values for the n-octyl and n-nonyl barbituric acid homologues). One possibility is that equilibrium has not been attained at the end of the *in vitro* incubation. Although there seems minimal evidence for this, it may be that diffusion processes for these highly lipophilic compounds are so slow that the time course used here is insufficient to demonstrate this. Increasing the incubation time, however, would also lead to significant deterioration in the tissue and hence possible erroneous results.

Although adsorption to the container occurred increasingly with increase in lipophilicity, this is not expected to influence the estimation of *Kpu in vitro*, as the concentrations of compound in both tissue and medium were determined experimentally rather than either one being based on the difference between the total amount of compound added and that in the tissue or medium, if only one of these had been measured. The underestimate in *Kpu* due to albumin diffusion during *in vitro* incubation for the current barbituric acid series was calculated to be approximately 20% for the n-nonyl homologue in muscle. Consequently, this alone also cannot explain the discrepancy between *in vitro* and *in vivo Kpu* values. It is likely that lipids and phospholipids, however, also diffuse from the tissue during *in vitro* incubations and, in combination with the albumin diffusion, this may well have a material influence on Kpu_e values for lipophilic compounds.

In Silico to *in Vivo* Correlation

Although the primary objective of this study was to evaluate an *in vitro* experiment method to predict *in vivo* tissue distribution, increasingly there is general interest in exploring the use of *in silico* approaches in ADME, which offer the promise of rapid prediction of pharmacokinetics, including tissue distribution coefficients, for a number of compounds in the early stages of drug discovery. Figure 4C shows the application of one general *a priori* prediction algorithm developed by Poulin and Theil (27,28), based on a com-

bination of the physicochemical properties of the compound (LogP, pKa, fraction unbound in plasma), and physiologic information, such as tissue water content and concentrations of neutral lipids and phospholipids, that has been reasonably successfully applied to a variety of compounds. Here, it is seen that the correlation is quite good, although the algorithm tended to overpredict *Kpu* (1.4-fold on average), with 35 out of the 90 predicted values being greater than 2-fold higher than the measured *in vivo Kpu,* and these associated primarily with the pentyl to nonyl homologues; only one predicted less than half the measured value.

Use of Kpu_e Values

Within the context of PBPK modeling, *Kp* values and plasma protein binding estimations are essential for the prediction of volume of distribution of drugs in individual tissues, and hence in the body as a whole. Kpu_e values are also helpful in dynamic modeling when vascular or cellular permeability do not limit the rate of tissue distribution. Under such conditions, when vascular perfusion is the rate-limiting step with respect to radial distribution from the vasculature, Kpu_e values have direct relevance. Such values have much more limited utility however, for drugs whose tissue distribution is permeability rate limited. Then the kinetic events occurring in each tissue space (vascular, interstitial, and cellular) must be considered separately to accurately characterize the global events in tissues (29). For such compounds, current *in vitro* tissue methodologies generally do not provide the necessary information.

CONCLUSION

The *in vitro* methodology developed resulted in a good prediction of *in vivo* Kpu_e values for a homologous series of 5-n-alkyl-5-ethyl barbituric acid derivatives over a wide range of lipophilicity. The *in vitro* Kpu_e values of the most lipophilic barbiturates, however, generally underpredicted those observed *in vivo*. This indicated that there are some issues with using the technique generically to predict *in vivo* distribution. For the barbiturates, the underprediction of *in vivo* Kpu_e may be attributed to a combination of binding to albumin and partitioning to lipids that had diffused from the tissue piece into the media or insufficient incubation time to allow a true equilibrium to be attained.

ACKNOWLEDGMENTS

The authors thank Dr Ivan Nestorov for the calculation of the dosing schemes for the barburates, and also acknowledge the assistance of Dr Eddie Clayton in developing the HPLC-MS-MS conditions and analyzing sample extracts for barbiturate concentration from the constant-rate i.v. infusion study. Peter Ballard would like to thank AstraZeneca for financial support.

REFERENCES

1. H.-S. G. Chen and J. F. Gross. Estimation of tissue-to-plasma partition coefficients used in physiological pharmacokinetic models. *J. Pharmacokinet. Biopharm.* **7**:117–125 (1979).
2. K. B. Bischoff, R. L. Dedrick, and D. S. Zaharko. Preliminary model for methotrexate pharmacokinetics. *J. Pharm. Sci.* **59**:149–154 (1970).
3. A. Benareggi and M. Rowland. Physiologic modeling of cyclosporin kinetics in rat and man. *J. Pharmacokinet. Biopharm.* **19**: 21–50 (1991).
4. J. L. Gabrielsson, L. K. Paalzow, and L. Nordstrom. A physiologically based pharmacokinetic model for theophylline disposition in the pregnant and nonpregnant rat. *J. Pharmacokinet. Biopharm.* **12**:149–165 (1984).
5. L. Granero, J. Chesa-Jimenez, V. Monserrat, M. Almela, M.-J. Gimeno, F. Torres-Molina, and J.-E. Peris-Ribera. Physiological pharmacokinetic model for ceftazidime disposition in the rat and its application to prediction of plasma concentration in humans. *Eur. J. Pharm. Sci.* **1**:3–11 (1993).
6. Y. Igari, Y. Sugiyama, S. Awazu, and M. Hanano. Comparative physiologically based pharmacokinetics of hexobarbital, phenobarbital and thiopental in the rat. *J. Pharmacokinet. Biopharm.* **10**:53–75 (1982).
7. G. E. Blakey, I. A. Nesterov, P. A. Arundel, L. J. Aarons, and M. Rowland. Quantitative structure pharmacokinetics relationships: 1. Development of a whole-body physiologically based model to characterize changes in pharmacokinetics across a homologous series of barbiturates in the rat. *J. Pharmacokinet. Biopharm.* **25**:277–312 (1997).
8. R. Gubser, C. DiFransesco, and M. H. Bickel. Uptake of lipophilic model compounds into the isolated perfused rat epididymal adipose tissue. *J. Pharmacol. Exp. Therap.* **237**:967–971 (1986).
9. C.-H. Chou, A. M. Evans, G. Fornasini, and M. Rowland. Relationship between lipophilicity and hepatic dispersion and distribution for a homologous series of barbiturates in the isolated perfused *in situ* rat liver. *Drug Metab. Dispos.* **21**:933–938 (1993).
10. A. Heatherington and M. Rowland. Estimation of reference spaces in the perfused rat hindlimb. *Eur. J. Pharm. Sci.* **2**:261–270 (1994).
11. M. H. Bickel, R. M. Raaflaub, M. Hellmuller, and E. J. Stauffer. Characterization of drug distribution and binding competition by two-chamber and multi-chamber distribution dialysis. *J. Pharm. Sci.* **76**:68–74 (1987).
12. T. M. Ludden, L. S. Schanker, and R. C. Lanman. Binding of organic compounds to rat liver and lung. *Drug Metab. Dispos.* **4**:8–16 (1976).
13. M. H. Bickel and J. W. Steele. Binding of basic and acidic drugs to rat tissue subcellular fractions. *Chemico-Biol. Int.* **8**:151–162 (1974).
14. W. O. Berndt. Use of the tissue slice technique for evaluation of renal transport processes. *Env. Health Persp.* **15**:73–88 (1976).
15. R. Drew and Z. H. Siddik. Effect of a specific 5HT uptake inhibitor (citalopram) on drug accumulation by rat lung slices. *Pharmacol.* **20**:27–31 (1980).
16. C. Post, R. G. G. Andersson, A. Ryrfeldt, and E. Nilsson. Transport and binding of lidocaine by lung slices and perfused lung of rats. *Acta Pharmacol. Tox.* **43**:156–163 (1978).
17. P. Ballard, P. A. Arundel, D. E. Leahy, and M. Rowland. Prediction of *in vivo* tissue distribution from *in vitro* data 2. Influence of albumin diffusion from tissue slices during an *in vitro* incubation on estimated tissue-to-unbound plasma partition coefficients (Kpu). *Pharm. Res.* **20**:857–863.
18. P. Ballard, D. E. Leahy, and M. Rowland. Prediction of *in vivo* tissue distribution from *in vitro* data. 1. Experiments with markers of aqueous spaces. *Pharm. Res.* **17**:660–663 (2000).
19. S. Toon and M. Rowland. Structure-pharmacokinetic relationships among the barbiturates in the rat. *J. Pharmacol. Exp. Ther.* **225**:752–763 (1983).
20. G. Blakey. Whole body tissue distribution of the 5-alkyl-5-ethyl barbituric acids in the rat (preliminary results). PhD thesis, University of Manchester, 1993.
21. S. H. Steiner, M. J. Moor, and M. H. Bickel. Kinetics of distribution and adipose tissue storage as a function of lipophilicity and chemical structure. I. Barbiturates. *Drug Metab. Dispos.* **19**: 8–14 (1991).
22. C. B. Frederick, D. W. Potter, M. I. Chang-Mateu, and M. E. Andersen. A physiologically-based pharmacokinetic and pharmacodynamic model to describe the oral dosing of rats with ethyl acrylate and its implications for risk assessment. *Tox. Appl. Pharmacol.* **114**:246–260 (1992).
23. V. Fiserova-Bergerova, M. Tichy, and F. J. Di Carlo. Effects of biosolubility on pulmonary uptake and disposition of gases and

vapors of lipophilic chemicals. *Drug Metab. Rev.* **15**:1033–1070 (1984).
24. J. H. Lin, Y. Sugiyama, S. Awazu, and M. Hanano. *In vitro* and *in vivo* evaluation of the tissue blood partition coefficient for physiological pharmacokinetic models. *J. Pharmacokinet. Biopharm.* **10**:637–647 (1982).
25. H. Harashima, Y. Sugiyama, Y. Sawada, T. Iga, and M. Hanano. Comparison between *in vivo* and *in vitro* tissue-to-plasma unbound concentration ratios ($K_{p,f}$) of quinidine in rats. *J. Pharm. Pharmacol.* **36**:340–342 (1984).
26. G. Schuhmann, B. Fichtl, and H. Kurz. Prediction of drug distribution *in vivo* on the basis of *in vitro* binding data. *Biopharm. Drug Dispos.* **8**:73–86 (1987).
27. P. Poulin and F.-P. Theil. Prediction of pharmacokinetics prior to *in vivo* studies. I. Mechanism-based prediction of volume of distribution. *J. Pharm. Sci.* **91**:129–156 (2002).
28. P. Poulin and F.-P. Theil. Prediction of pharmacokinetics prior to *in vivo* studies. II. Generic physiologically based pharmacokinetic models of drug disposition. *J. Pharm. Sci.* **91**:1358–1370 (2002).
29. I. Nestorov, L. J. Aarons, and M. Rowland. Quantitative structure-pharmacokinetics relationships: II. A mechanistically based model to evaluate the relationship between tissue distribution parameters and compound lipophilicity. *J. Pharmacokinet. Biopharm.* **26**:521–545 (1998).
30. T. D. Yih and J. M. van Rossum. Ks values of some homologous series of barbiturates and the relationship with the lipophilicity and metabolic clearance. *Biochem. Pharmacol.* **26**:2117–2120 (1977).
31. C. Hansch, A. R. Steward, S. M. Anderson, and D. Bentley. The parabolic dependence of drug action upon lipophilic character as revealed by a study of hypnotics. *J. Med. Chem.* **11**:1–11 (1967).